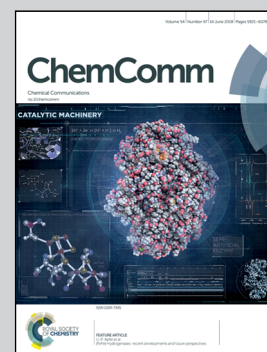


Showcasing research from Professor Yun Yan's laboratory,
College of Chemistry and Molecular Engineering,
Peking University, Beijing, China.

Self-assembly facilitated and visible light-driven generation
of carbon dots

Molecular self-assembly may act as important precursor
for generation of carbon dots! Visible light irradiation of
self-assembled terthiophene amphiphile TTC4L triggers
the production of superoxide radical in water which
oxidizes the closely packed terthiophene group into
carbon dots.

As featured in:



See Yun Yan *et al.*,
Chem. Commun., 2018, 54, 5960.



Self-assembly facilitated and visible light-driven generation of carbon dots†

Cite this: *Chem. Commun.*, 2018, 54, 5960

Received 23rd November 2017,
Accepted 21st April 2018

DOI: 10.1039/c7cc08876k

rsc.li/chemcomm

Tian Huang,^{ab} Tongyue Wu,^a Zhiyang Zhu,^a Li Zhao,^{id c} Haina Ci,^b Xuedong Gao,^a Kaerdun Liu,^a Junfang Zhao,^d Jianbin Huang^{ab} and Yun Yan^{id *a}

Carbon dots (CDs) with an absolute fluorescence quantum yield of 87% are facily prepared *via* irradiation of self-assembled terthiophene amphiphile TTC4L in aqueous solution by mild visible light. Visible light irradiation of TTC4L triggers the production of superoxide radicals in water, which oxidize the closely packed terthiophene group into carbon dots. Our results reveal that the molecular self-assembly may act as important precursor for the generation of single molecule-like carbon dots; this method paves the way for the fabrication of CDs of high quality.

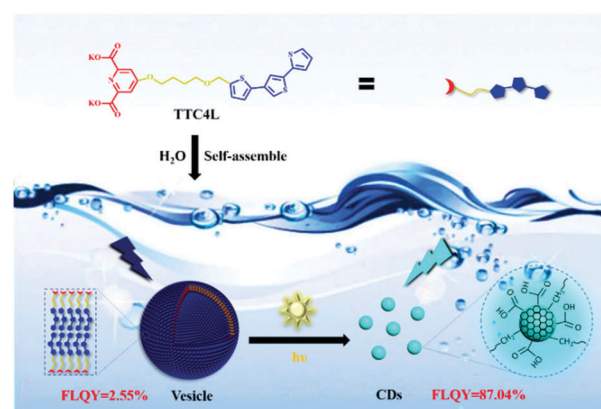
Recent decades have witnessed the rapid development of molecular self-assemblies owing to their potential applications in the fabrication of advanced materials,^{1–4} especially in the fabrication of various smart materials, which are responsive to external stimuli such as light, temperature, and pH.^{5–7} Besides the responsiveness of the molecular self-assemblies, the ordered molecular arrangement is also very useful in material science, for example, creating conductive materials,⁸ chiral self-assembled structures,⁹ and various supramolecular polymers.^{10,11} However, so far, the advantages of ordered molecular arrangements in molecular self-assemblies have seldom been exploited in the preparation of carbon dots (CDs).

As prospective nanomaterials, CDs have attracted intensive attention in the field of solar energy conversion,^{12–14} bio-imaging^{15,16} as well as chemical sensing^{17,18} owing to their stable photoluminescence (PL), low cytotoxicity, and excellent biocompatibility. CDs are essentially ultrasmall fragments of carbon materials with tunable degrees of carbonization, and they are usually fabricated from carbon soot, graphite or carbon nanotubes *via* arc discharge,¹⁹

laser ablation,²⁰ or electrochemical oxidation.²¹ Molecular precursors are also widely employed to obtain CDs, where small molecules are treated with hydrothermal²² or solvothermal²³ cutting strategies, or they are subjected to microwave pyrolysis,²⁴ which finally results in the formation of nanometer-sized carbon materials.

In this study, we show that molecular self-assembly can facilitate generation of CDs under visible light irradiation. In contrast to literature methods that require high voltage, temperature, strong acids or involve the use of special equipment, visible light irradiation of the vesicular self-assembly of terthiophene amphiphile TTC4L in water can generate CDs with an absolute fluorescence quantum yield up to 87%. Mechanism study shows that photo-induced generation of superoxide radicals ($O_2^{\cdot-}$) triggers the carbonization of the terthiophene moiety, which finally leads to the generation of CDs. This study for the first time reports the advantage of using molecular self-assembly as a precursor for the fabrication of carbon dots and the possibility of generating carbon dots with visible light irradiation (Scheme 1).

TTC4L was synthesized in our lab;²⁵ it is an amphiphile with a terthiophene group in the hydrophobic tail tethered to a hydrophilic chelidamic acid head *via* an oxyl-butyl chain (Scheme 1). This molecule was able to self-assemble into vesicles in water, and the



Scheme 1 Illustration for the formation of TTC4L-CDs.

^a Beijing National Laboratory for Molecular Sciences, Institution College of Chemistry and Molecular Engineering, Peking University, Beijing, 100871, China

^b Academy for Advanced Interdisciplinary Studies, Peking University, Beijing 100871, China

^c School of Food and Chemical Engineering, Beijing Technology and Business University, Beijing 100048, China

^d Technical Institute of Physics and Chemistry, Chinese Academy of Science, Beijing 100190, China. E-mail: yunyan@pku.edu.cn

† Electronic supplementary information (ESI) available. See DOI: 10.1039/c7cc08876k

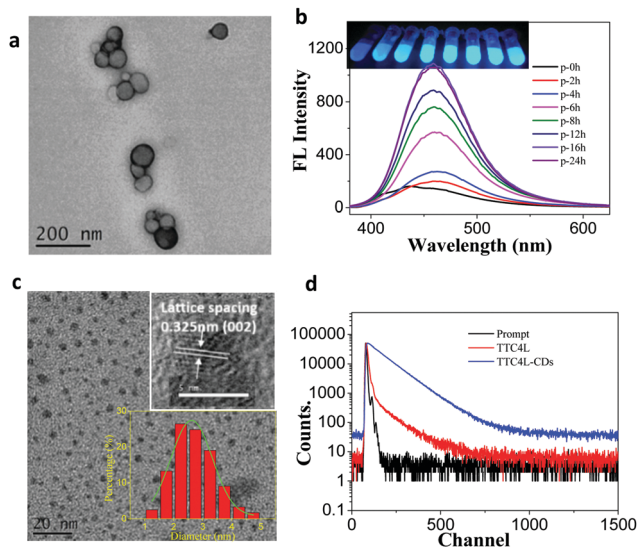


Fig. 1 (a) TEM image of vesicles formed in 50 μM TTC4L. (b) Fluorescence spectra of 50 μM TTC4L aqueous solution irradiated by a daylight lamp (25 mW cm^{-2}) at different times. Inset: Photos of the solution at different irradiation time under 365 UV (from left to right). (c) TEM image of CDs (upper inset: high resolution image of CDs; lower inset: size distribution of CDs). (d) Fluorescence lifetime of TTC4L and CDs.

size of the TTC4L vesicles was concentration-dependent.²⁵ In the present study, vesicles with a diameter in the range of 60–90 nm were formed in the 50 μM TTC4L aqueous solution (Fig. 1a). The vesicular suspension of TTC4L emitted blue emission (Fig. 1b, black line) at 435 nm. However, the fluorescence shifted to 460 nm, and its intensity increased continuously (Fig. 1b) upon irradiation with a daylight lamp (25 mW cm^{-2}). After 16 hours, the fluorescence intensity reached maximum, which was about 5 folds of the original intensity, and the absolute FLQY amount as high as 87% was obtained. Meanwhile, the UV absorbance of TTC4L decreased (Fig. S1, ESI[†]). ¹H NMR measurements revealed the disappearance of signals corresponding to the terthiophene group, indicating that TTC4L had undergone a photochemical reaction (Fig. S2, ESI[†]). TEM images revealed the formation of small nanoparticles with an average diameter of $2.7 \pm 0.4 \text{ nm}$ (Fig. 1c, lower inset). A lattice spacing of 0.32 nm was correlated with the distance of the (002) facet of graphitic carbon,^{26,27} and it was obtained with high resolution TEM (Fig. 1c, upper inset), indicating the formation of carbon dots (denoted as TTC4L-CDs). AFM measurements showed the average topographic height of the obtained carbon dots to be about $1.6 \pm 0.3 \text{ nm}$ (Fig. S3, ESI[†]). The ultra-high fluorescence quantum yield was attributed to the presence of the light-generated carbon dots. Fig. 1d reveals that TTC4L-CDs displayed a single exponential fluorescence lifetime of 2.5 ns, which was significantly different from the two lifetimes observed for the original TTC4L vesicles (Fig. 1d and Table S1, ESI[†]).

FLQY is usually closely related to the composition and surface groups of CDs.^{28,29} X-ray photoelectron spectroscopy (XPS) results (Fig. 2a) indicate that CDs are mainly composed of carbon and oxygen, with small amounts of nitrogen and sulphur. It is worth noting that the peak intensities of nitrogen and sulphur in the original TTC4L solution are much stronger

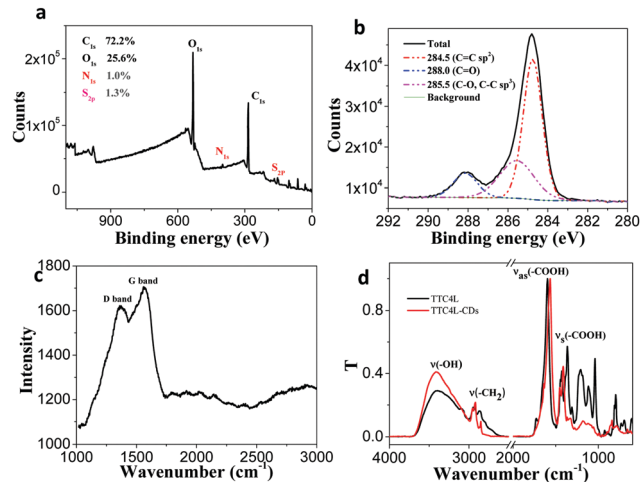


Fig. 2 Surface-state characterizations of TTC4L-CDs. (a) XPS spectrum of TTC4L-CDs. (b) High-resolution of C1s of XPS spectrum. (c) Raman spectrum of TTC4L-CDs. (d) FT-IR spectra of TTC4L and TTC4L-CDs.

than those of the irradiated sample (Fig. S4, ESI[†]), suggesting that the nitrogen and sulphur levels are significantly reduced in CDs following light-irradiation. XPS measurements for the samples at different irradiating stages (Fig. S5, ESI[†]) reveal that the contents of the original $\text{S}_{2\text{p}}$ at 163.9 eV and $\text{N}_{1\text{s}}$ at 399.0 eV of TTC4L decrease with the increasing irradiation time. Meanwhile, a new peak at 168.2 eV (S element in sulfur dioxide) for $\text{S}_{2\text{p}}$ and a new peak at 401.1 eV (N element in ammonium compound) for $\text{N}_{1\text{s}}$ occur, suggesting a progressive photo-oxidation process of TTC4L. The high-resolution XPS spectrum for the final purified TTC4L-CDs can be resolved into 3 main peaks from different binding states of $\text{C}_{1\text{s}}$ electrons (Fig. 2b): the one at 284.5 eV can be assigned to the graphitic skeleton ($\text{sp}^2 \text{ C-C}$), whereas the one at 285.5 eV indicates the presence of C–O bond and the C–C single bond, and the peak at 288.0 eV signalizes C=O bond.

The surface state of TTC4L-CDs was further examined using Raman and FT-IR measurements. The Raman spectrum revealed that CDs displayed D and G bands at 1365 and 1570 cm^{-1} , respectively (Fig. 2c), which is a characteristic of carbon materials. The relative intensity ratio of the D-band and the crystalline G-band ($I_{\text{D}}/I_{\text{G}}$) was about 0.9, which is a very large value indicating the presence of considerable defects.^{30,31} Furthermore, FT-IR spectra (Fig. 2d) exhibited that the skeletal vibration of the pyridine ring at 1370 cm^{-1} , the C–O–C asymmetric and symmetric stretching vibrations at 1100 and 1040 cm^{-1} , respectively, and the out-of-plane vibration of aromatic rings at 800 cm^{-1} nearly vanished for TTC4L-CDs. However, the symmetric and asymmetric stretching vibrations of C=O around 1409 cm^{-1} and 1565 cm^{-1} , respectively, were still observed, but the separation between the symmetric and asymmetric vibrations decreased by about 100 cm^{-1} , suggesting that the environment of C=O had changed drastically. Meanwhile, a broad vibrational band for a hydrogen bond was observed at 3410 cm^{-1} . These IR features suggested the presence of –COOH groups on the surface of CDs. Indeed, CDs displayed reversible pH-dependent fluorescence. The fluorescence decreased as the pH

decreased, which was probably due to the hydrogen bonding between CDs (Fig. S6, ESI[†]). Specially, the asymmetric and symmetric vibrations for $-\text{CH}_2-$ were also observed at 2921 cm^{-1} and 2850 cm^{-1} , respectively, indicating that the hydrophobic carbon chain of TTC4L was probably attached to the surface of CDs. It is possible that both the $-\text{COOH}$ groups and the pending alkyl chains are beneficial for high FLQY of TTC4L-CDs through a surface passivation mechanism.^{20,28,29}

Unlike most CDs, which display excitation-dependent emission,^{32,33} TTC4L-CDs display excitation-independent emission. As the excitation wavelength varies from 254 nm to 380 nm, the maximum emission wavelength remains constant (Fig. S7a, ESI[†]), suggesting that the emission originates from defects rather than from the band-gaps.^{20,34} This is in line with the large I_D/I_G value obtained in the Raman measurement (Fig. 2c). The defect-facilitated emission of TTC4L-CDs have a narrow full width at half-maximum (FWHM) of only 70 nm (Fig. S7b, ESI[†]), which is narrower than most of the FWHM values of $>100\text{ nm}$ for other CDs.³¹ By combining these results with the single exponential decay of the fluorescence lifetime, we infer that single molecule-like CDs have been generated with light in this study.

Excitingly, the single molecule-like CDs display two-photon fluorescence properties. Fig. 3a reveals that upon exposure to a near-infrared (NIR) femtosecond laser of 730 nm, TTC4L-CDs exhibit emission as well. With the logarithmic coordinates, the linear slope observed is 1.89, which describes a clear quadratic relationship between the excitation laser power and the fluorescence intensity (Fig. 3b), confirming that excitation with two NIR photons is responsible for the fluorescence of CDs.³⁵

To gain more insight into the formation mechanism of TTC4L-CDs, time-resolved transient absorption (TRTA) spectroscopy was employed to study the intermediate species generated in the photo-irradiation process. The characteristic peak of the terthiophene group at the triplet state ($^3\text{TTC4L}^*$)³⁶ located at 452 nm was observed (Fig. 4a). The lifetime of $^3\text{TTC4L}^*$ was about $2.12\text{ }\mu\text{s}$ (Fig. S8, ESI[†]), which meant that the excited triplet TTC4L ($^3\text{TTC4L}^*$) may have sufficient lifetime to transfer its energy to a triplet oxygen to generate ROS. Indeed, as the TTC4L aqueous solution was exposed to light, a typical electron paramagnetic resonance (EPR) signal (Fig. 4b, red line) was observed using BMPO as the radical trap. The simulated result (Fig. 4b, blue line) of the EPR signal was consistent with that of

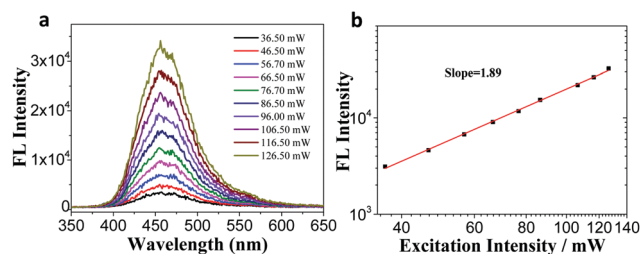


Fig. 3 (a) Two-photon spectra of TTC4L-CDs at different laser excitation intensities of 730 nm femtosecond pulse laser. (b) Relationship between the two-photon emission intensity and laser excitation intensity.

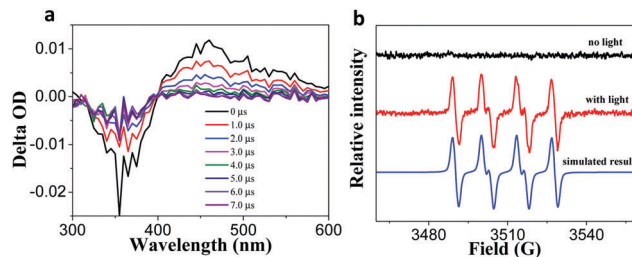


Fig. 4 (a) Time-resolved transient spectra of TTC4L aqueous solution under 355 nm pump light. (b) Electron paramagnetic resonance spectra of TTC4L aqueous solution by adding BMPO as a radical trap agent.

the $\text{O}_2^{\bullet-}$ signal. Control experiments suggested that no EPR signal could be observed in the TTC4L aqueous system without exposure to light (Fig. 4b, black line), indicating that $\text{O}_2^{\bullet-}$ was generated by irradiating the TTC4L aqueous system with visible light. The production of $\text{O}_2^{\bullet-}$ is very crucial in the visible light-generated CDs. As a proof of this argument, when the reactive $\text{O}_2^{\bullet-}$ was consumed due to the degradation of organic dyes, such as rhodamine B, the fluorescence of TTC4L only increased slightly, (Fig. S9, ESI[†]), confirming the important role of $\text{O}_2^{\bullet-}$ in the formation of CDs.

The self-assembling ability of TTC4L is very crucial in the light-triggered generation of CDs. Upon dissolving TTC4L in a good solvent such as ethanol, the fluorescence only slowly increased by 1-fold after 24 hours of irradiation (Fig. S10, ESI[†]). However, as the hydrocarbon chain tethering the coordinating head and the terthiophene group is extended from 4 $-\text{CH}_2-$ (TTC4L) to 8 $-\text{CH}_2-$ to enhance the self-assembling ability of the terthiophene moiety (TTC8L, Fig. 5a), the CDs could be generated more rapidly. Fig. 5b shows the UV-vis spectra of TTC4L and TTC8L aqueous solutions; the stronger aggregation ability of TTC8L than that of TTC4L led to the increase in turbidity. In Fig. 5c and Fig. S11 (ESI[†]), we show that the fluorescence reaches a maximum within 12 hours in the TTC8L system, whereas it reaches a maximum in 16 hours in the TTC4L system. In contrast to the 60–90 nm vesicles formed by TTC4L, the formation of hexagonal structures of 2400 nm long and 500 nm in width was revealed by TEM observations for the TTC8L system

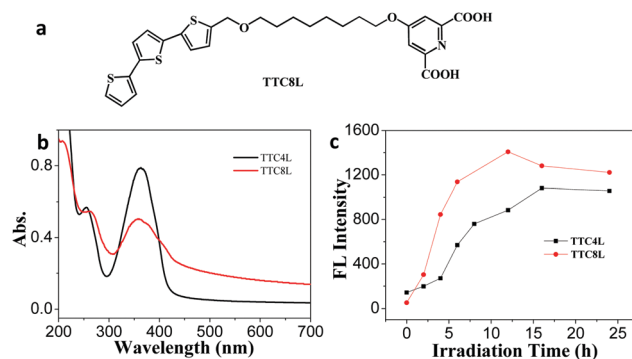


Fig. 5 (a) Chemical structure of TTC8L. (b) UV-vis spectra of TTC4L and TTC8L aqueous solutions. (c) Fluorescence intensities of TTC4L and TTC8L aqueous solutions with longer light irradiation times.

(Fig. S12a, ESI[†]). However, the size and emission of CDs obtained for the TTC8L system were the same as those obtained for the TTC4L system (Fig. S12b, ESI[†]), indicating that the size and morphology of the self-assembled structure did not impact the final properties of CDs. Finally, the amphiphilic structure of TTC4L was important in the formation of CDs. Control experiments suggested that no CDs were formed when terthiophene (TT) was simply dispersed in water under the same irradiation conditions; although it is insoluble and forms 'aggregates', no obvious fluorescence enhancement was observed (Fig. S12, ESI[†]). It is possible that self-assembly facilitates facile diffusion of oxygen into the terthiophene arrays, which triggered the carbonization of the TTC4L molecules.

In summary, we report the first case of visible light-generated carbon dots in the molecular self-assembly of terthiophene amphiphile TTC4L. The resultant CDs display narrow size distribution, which endows them with excitation-independent emission and two-photon emission. The absolute fluorescence quantum yield of these CDs can be as high as *ca.* 87%, which is probably owing to the presence of alkyl chains and COOH groups on the surface as a result of mild photo-reaction. Mechanism study shows that visible light irradiation facilitates the formation of long-lived TTC4L triplets, which transfer their energy to oxygen to produce O₂^{•−}. The reactive O₂^{•−} radical triggers carbonization of the terthiophene skeleton in the self-assembly of TTC4L. Although the details for the carbonization are still not clear, we believe that the close arrangement of the terthiophene group in the self-assembly of TTC4L is very crucial in the CD formation, which allows facile generation of C–C bonds. In conclusion, the present visible light-driven strategy provides a new approach to prepare high quality CDs, which are promising for a diverse range of applications such as solar energy conversion and bioimaging.

This study is supported by the National Natural Science Foundation of China (Grant No. 21573011), and National Basic Research Program of China (2013CB933800).

Conflicts of interest

There are no conflicts to declare.

Notes and references

- 1 Y. Yan, L. Jiang and J. Huang, *Phys. Chem. Chem. Phys.*, 2011, **13**, 9074–9082.
- 2 Y. Yan and J. Huang, *Coord. Chem. Rev.*, 2010, **254**, 1072–1080.
- 3 Y. Liu, B. Liu and Z. Nie, *Nano Today*, 2015, **10**, 278–300.
- 4 Q. Zhao, Y. Wang, Y. Yan and J. Huang, *ACS Nano*, 2014, **8**, 11341–11349.
- 5 Z. Wu, Y. Yan and J. Huang, *Langmuir*, 2014, **30**, 14375–14384.
- 6 A. Wang, W. Shi, J. Huang and Y. Yan, *Soft Matter*, 2016, **12**, 337–357.
- 7 H. Yang, B. Yuan, X. Zhang and O. A. Scherman, *Acc. Chem. Res.*, 2014, **47**, 2106–2115.
- 8 Y. Che, A. Datar, X. Yang, T. Naddo, J. Zhao and L. Zang, *J. Am. Chem. Soc.*, 2007, **129**, 6354–6355.
- 9 Z. Shen, T. Wang and M. Liu, *Angew. Chem., Int. Ed.*, 2014, **53**, 13424–13428.
- 10 L. Brunsveld, B. Folmer, E. W. Meijer and R. Sijbesma, *Chem. Rev.*, 2001, **101**, 4071–4098.
- 11 T. Aida, E. Meijer and S. Stupp, *Science*, 2012, **335**, 813–817.
- 12 J. Briscoe, A. Marinovic, M. Sevilla, S. Dunn and M. Titirici, *Angew. Chem., Int. Ed.*, 2015, **54**, 4463–4468.
- 13 G. A. M. Hutton, B. Reuillard, B. C. M. Martindale, C. A. Caputo, C. W. J. Lockwood, J. N. Butt and E. Reisner, *J. Am. Chem. Soc.*, 2016, **138**, 16722–16730.
- 14 B. C. M. Martindale, E. Joliat, C. Bachmann, R. Alberto and E. Reisner, *Angew. Chem., Int. Ed.*, 2016, **55**, 9402–9406.
- 15 S.-T. Yang, L. Cao, P. G. Luo, F. Lu, X. Wang, H. Wang, M. J. Meziani, Y. Liu, G. Qi and Y.-P. Sun, *J. Am. Chem. Soc.*, 2009, **131**, 11308–11309.
- 16 Y. Song, C. Zhu, J. Song, H. Li, D. Du and Y. Lin, *ACS Appl. Mater. Interfaces*, 2017, **9**, 7399–7405.
- 17 S.-W. Hu, S. Qiao, B.-Y. Xu, X. Peng, J.-J. Xu and H.-Y. Chen, *Anal. Chem.*, 2017, **89**, 2131–2137.
- 18 X. Gao, C. Du, Z. Zhuang and W. Chen, *J. Mater. Chem. C*, 2016, **4**, 6927–6945.
- 19 X. Xu, R. Ray, Y. Gu, H. J. Ploehn, L. Gearheart, K. Raker and W. A. Scrivens, *J. Am. Chem. Soc.*, 2004, **126**, 12736–12737.
- 20 Y.-P. Sun, B. Zhou, Y. Lin, W. Wang, K. A. S. Fernando, P. Pathak, M. J. Meziani, B. A. Harruff, X. Wang, H. Wang, P. G. Luo, H. Yang, M. E. Kose, B. Chen, L. M. Veca and S.-Y. Xie, *J. Am. Chem. Soc.*, 2006, **128**, 7756–7757.
- 21 J. Zhou, C. Booker, R. Li, X. Zhou, T.-K. Sham, X. Sun and Z. Ding, *J. Am. Chem. Soc.*, 2007, **129**, 744–745.
- 22 Z. Liang, M. Kang, G. F. Payne, X. Wang and R. Sun, *ACS Appl. Mater. Interfaces*, 2016, **8**, 17478–17488.
- 23 M. Zheng, Y. Li, S. Liu, W. Wang, Z. Xie and X. Jing, *ACS Appl. Mater. Interfaces*, 2016, **8**, 23533–23541.
- 24 H. Zhu, X. Wang, Y. Li, Z. Wang, F. Yang and X. Yang, *Chem. Commun.*, 2009, 5118–5120, DOI: 10.1039/b907612c.
- 25 L. Zhao, X. Cheng, Y. Ding, Y. Yan and J. Huang, *Soft Matter*, 2012, **8**, 10472–10478.
- 26 X. Wu, J. Zhao, S. Guo, L. Wang, W. Shi, H. Huang, Y. Liu and Z. Kang, *Nanoscale*, 2016, **8**, 17314–17321.
- 27 L. Bai, S. Qiao, Y. Fang, J. Tian, J. McLeod, Y. Song, H. Huang, Y. Liu and Z. Kang, *J. Mater. Chem. C*, 2016, **4**, 8490–8495.
- 28 M. Zheng, Z. G. Xie, D. Qu, D. Li, P. Du, X. B. Jing and Z. C. Sun, *ACS Appl. Mater. Interfaces*, 2013, **5**, 13242–13247.
- 29 P. Anilkumar, X. Wang, L. Cao, S. Sahu, J. H. Liu, P. Wang, K. Korch, K. N. Tackett, A. Parenzan and Y. P. Sun, *Nanoscale*, 2011, **3**, 2023–2027.
- 30 M. R. Ammar, N. Galy, J. N. Rouzaud, N. Toulhoat, C. E. Vaudey, P. Simon and N. Moncoffre, *Carbon*, 2015, **95**, 364–373.
- 31 L. Bao, C. Liu, Z. L. Zhang and D. W. Pang, *Adv. Mater.*, 2015, **27**, 1663–1667.
- 32 L. Pan, S. Sun, A. Zhang, K. Jiang, L. Zhang, C. Dong, Q. Huang, A. Wu and H. Lin, *Adv. Mater.*, 2015, **27**, 7782–7787.
- 33 L. Ge, H. Yu, H. Ren, B. Shi, Q. Guo, W. Gao, Z. Li and J. Li, *J. Mater. Sci.*, 2017, **52**, 9979–9989.
- 34 Y. Mu, N. Wang, Z. C. Sun, J. Wang, J. Y. Li and J. H. Yu, *Chem. Sci.*, 2016, **7**, 3564–3568.
- 35 S. Lu, G. Xiao, L. Sui, T. Feng, X. Yong, S. Zhu, B. Li, Z. Liu, B. Zou, M. Jin, J. S. Tse, H. Yan and B. Yang, *Angew. Chem., Int. Ed.*, 2017, **56**, 6187–6191.
- 36 C. H. Evans and J. C. Scaiano, *J. Am. Chem. Soc.*, 1990, **112**, 2694–2701.